Electronic Supplementary Material (ESI) for Journal of Materials Chemistry C.

Supporting Information

Strong Upconversion Emission in $CsPbBr_3$ Perovskite Quantum Dots through Efficient $BaYF_5$: Yb, Ln Sensitization

Min Zeng[a,b], Shalini Singh[b], Zeger Hens[b], Jing Liu[a]*, Flavia Artizzu[a]*, Rik Van Deun[a]

[a]*L^3–Luminescent Lanthanide Lab, and* [b]*Physics and Chemistry of Nanostructures (PCN), Department of Chemistry, Ghent University, Krijgslaan 281-S3, 9000 Ghent, Belgium*

*Corresponding authors: Jing.Liu@UGent.be; Flavia.Artizzu@UGent.be

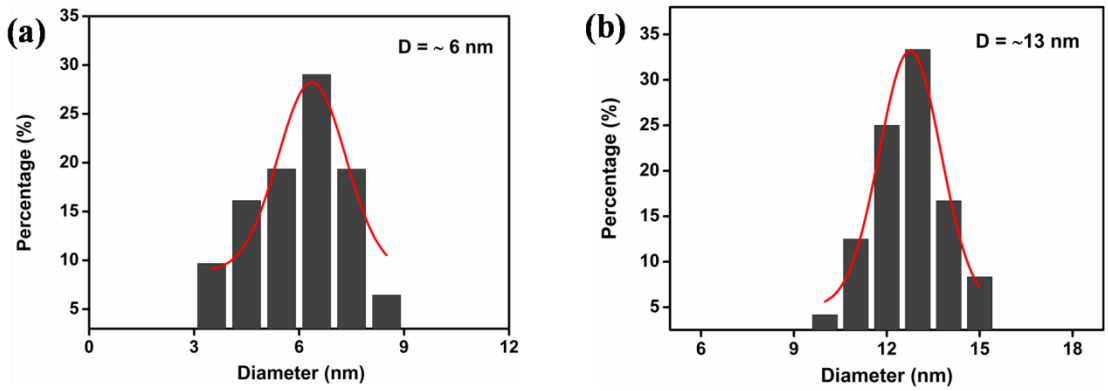

Fig. S1 Size distribution histograms of (a) $BaYF_5$: Yb, Tm UCNPs and (b) $CsPbBr_3$ QDs.

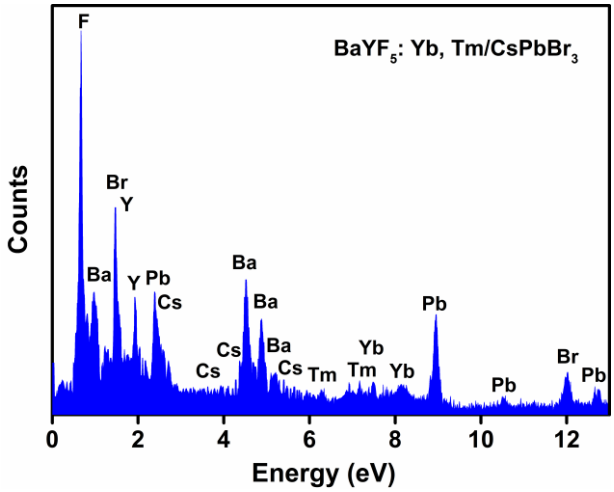

Fig. S2 EDX spectrum of the $BaYF_5$: Yb, Tm/$CsPbBr_3$ composite with 1: 1 ratio. The results are summarized in the following Table.

Table S1. EDX elemental analysis of the $BaYF_5$: Yb, Tm/$CsPbBr_3$ composite with 1: 1 ratio, indicating the existence of Ba, Y, F, Yb, Tm, Cs, Pb and Br elements which are assigned to $BaYF_5$: Yb, Tm UCNPs and $CsPbBr_3$ QDs. The value of lanthanide does not represent the actual composition because of instrument limitations.

Element	**Ba**	**Y**	**F**	**Yb**	**Tm**	**Cs**	**Pb**	**Br**
At %	8.02	6.4	35.45	0.95	0.42	8.26	9.88	30.63

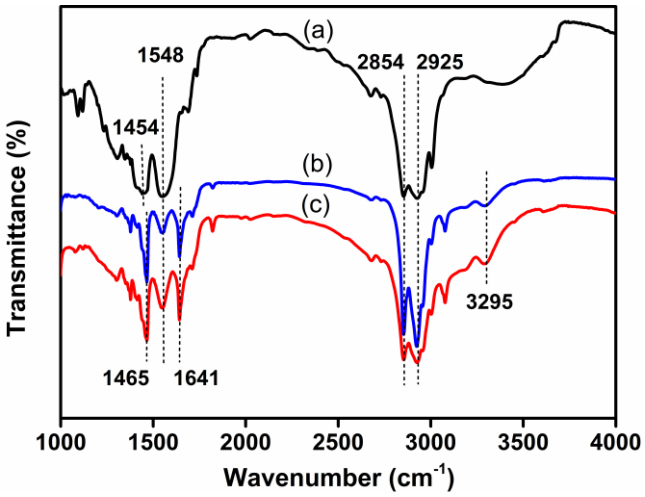

Fig. S3 FT-IR spectra of (a) $BaYF_5$: Yb, Tm UCNPs, (b) $CsPbBr_3$ QDs and (c) $BaYF_5$: Yb, Tm/$CsPbBr_3$ composite with 1: 0.25 ratio.

FT-IR spectra evidence a strong resemblance of the transmission bands appearing at 2925 and 2854 cm^{-1}, which are assigned to the asymmetric and symmetric stretching vibrations of methylene groups ($–CH_2$), respectively.[1] The bands at 1454 cm^{-1} in the spectrum of UCNPs (a) and 1548 cm^{-1} in the three spectra are attributed to the symmetric and antisymmetric stretching of the carboxylate (COO–), respectively. The result indicates that OA molecules were chemisorbed onto the UCNPs as a carboxylate.[2] In the spectra of $CsPbBr_3$ QDs (b) and $BaYF_5$: Yb, Tm/$CsPbBr_3$ composite (c), the characteristic peaks of OLA are observed at 1465, 1641, and 3295 cm^{-1}, which are associated with –C–H bending, C=O stretching and N–H stretching, respectively.[3–4] It is interesting to notice that the very broad shoulder at around 3400 cm^{-1}, related to the OH groups of OA in the spectrum of UCNPs (a), completely disappeared in the spectrum of the composite (c), indicating a thoroughly deprotonation of the carboxylic group in the presence of OLA, to form oleate.

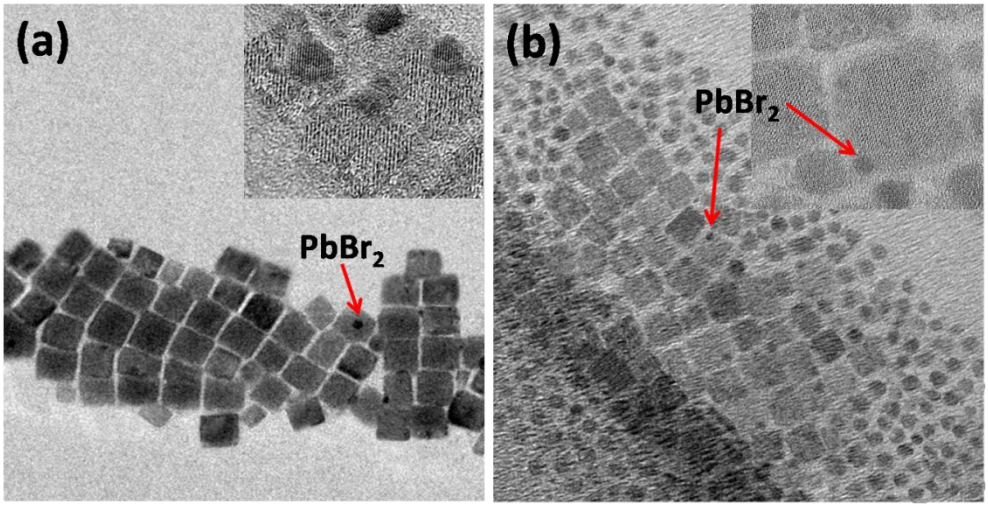

Fig. S4 TEM images of (a) $BaYF_5$: Yb, Tm/$CsPbBr_3$ composite with 1: 1 ratio synthesized through the *in-situ* growth method, (b) mixture of $BaYF_5$: Yb, Tm UCNPs and $CsPbBr_3$ QDs with 1: 1 ratio assembled by physical mixing. The red arrows indicate small black dots with poor crystallinity of about 2 nm which are attributed to $PbBr_2$ nanoparticles (coexisting along the $CsPbBr_3$ QDs[5]), which can be easily distinguished from UCNPs by different sizes and crystallinity.

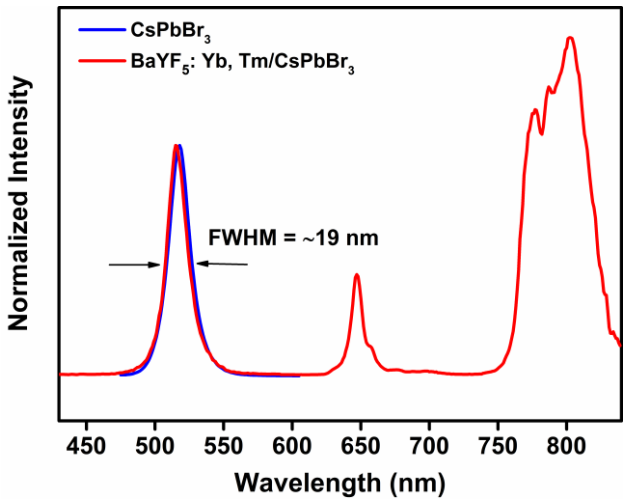

Fig. S5 Emission spectrum of the pristine $CsPbBr_3$ QDs excited at 466 nm (blue line), UCL emission spectrum of the $BaYF_5$: Yb, Tm/$CsPbBr_3$ QDs composite (red line) excited at 975 nm.

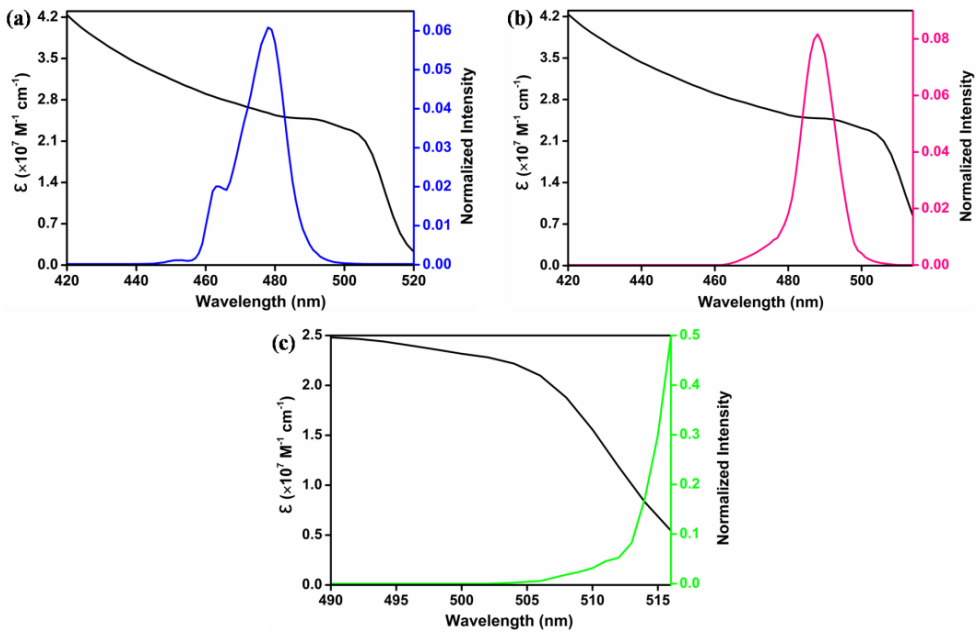

Fig. S6 Absorption spectra of $CsPbBr_3$ QDs (black line) and normalized UCL emission spectra of (a) $BaYF_5$: Yb, Tm (blue line), (b) $BaYF_5$: Yb, Ho (pink line), and (c) $BaYF_5$: Yb, Er (green line), which are used to calculate the overlap integral (J). There is partial spectral overlap between the $BaYF_5$: Yb, Er FRET donor and the $CsPbBr_3$ acceptor.

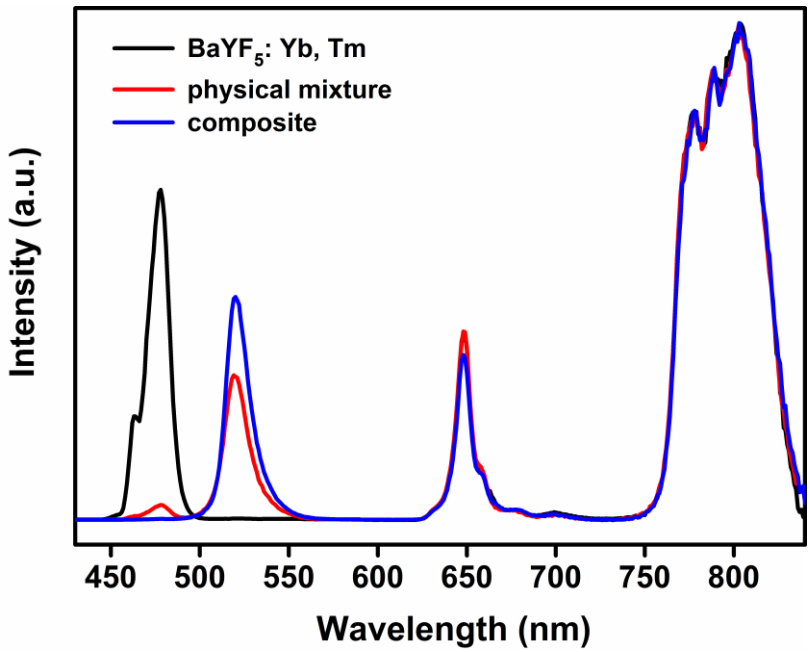

Fig. S7 UCL emission spectra of $BaYF_5$: Yb, Tm UCNPs (black line), $BaYF_5$: Yb, Tm/$CsPbBr_3$ QDs composite with 1: 1 ratio (blue line), physical mixture of $BaYF_5$: Yb, Tm and $CsPbBr_3$ QDs with the same composite ratio (red line).

Förster resonance energy transfer

The FRET efficiency can be experimentally estimated based on the corresponding decay lifetimes:[6]

$$\eta = 1 - \frac{\tau_{DA}}{\tau_D} \qquad \text{(S1)}$$

where τ_D and τ_{DA} are the luminescence lifetimes of the donor in the absence and presence of the acceptor, respectively.

Efficient FRET between UCNPs donors and $CsPbBr_3$ QDs acceptors will only take place at short distances.[7] The distance at which energy transfer efficiency is 50%, defined as the Förster radius (R_0), is given by:[8]

$$R_0 = \left[\frac{9(\mathit{In}10)\kappa^2 \phi_D}{128\pi^5 N_A n^4} J \right]^{1/6} \qquad \text{(S2)}$$

where κ^2 is the orientation factor of the interacting dipoles, Φ_D is the luminescence quantum yield of the donor in the absence of the acceptor, n is the average refractive index of the medium, N_A is the Avogadro constant, and J is a spectral overlap integral (M^{-1} cm^{-1} nm^4). The integral J can be defined as:[8]

$$J(\lambda) = \int F_D(\lambda) \varepsilon_A \lambda^4 \mathrm{d}\lambda \qquad \text{(S3)}$$

where $F_D(\lambda)$ is the UCL spectrum of the donor normalized to unit area ($\int F_D(\lambda)\, d\lambda = 1$), and ε_A is the acceptor's molar extinction coefficient (M^{-1} cm^{-1}) as a function of the wavelength λ (nm), as shown in Fig. S4. Herein, the value of 2/3 was used for κ^2 (assuming a random orientation of donor and acceptor dipoles), while $\kappa^2 = 4$ was also used to allow comparison across the literature. The refractive index of the medium was taken as 1.44, an average value between 1.427 (cyclohexane) and 1.459 (OA). The reported PLQY of the UCNPs donor (Φ_D) was in the range of 0.005-0.1%,[9] while $\Phi_D = 0.01\%$ was also assumed for the UCNPs to allow comparison across the literature.[10,11]

The rate of FRET (κ_T) is calculated from the lifetime of the donor in absence of the acceptor, Förster distance, and the average UCNPs-QDs separation distance, according to Eq. (S4):[12]

$$\kappa_T = \frac{1}{\tau_D} \times \left(\frac{R_0}{\mathrm{r}} \right)^6 \qquad \text{(S4)}$$

Taking into account an average separation distance between the donor and the acceptor of 3 nm (Ln ions in the center of the particle) and τ_D values reported in Table 1 in the manuscript (9.4 μs, 9.0 μs and 28.9 μs for Tm^{3+}, Ho^{3+} and Er^{3+}, respectively), it is possible to retrieve κ_T values of 2.7×10^5 s^{-1}, 2.9×10^5 s^{-1} and 3.4×10^4 s^{-1} for the FRET processes from the Tm^{3+}, Ho^{3+} and Er^{3+} donors, respectively.

It has however to be remarked that in the studied systems the donor units are the emitting lanthanide ions (Tm^{3+}, Ho^{3+} and Er^{3+}) that are homogeneously distributed into the UCNPs and therefore lie at various distances from the surface of the QDs acceptor depending on the size of the nanoparticle. According to the Förster's model, predictions of the FRET efficiency on dependence of the distance r between the donor/acceptor pair, can be quantified by the following equation:[7]

$$\eta = \frac{R_0^6}{R_0^6 + r^6} \qquad \text{(S5)}$$

As shown in Fig. S6, the FRET efficiencies estimated by the Förster model (taking the reliable value of κ^2 =2/3) can reach ~70% for the Tm^{3+} and Ho^{3+} to $CsPbBr_3$ QDs, and ~50% for Er^{3+} to $CsPbBr_3$ QDs when the Ln^{3+} are located in the center of the UCNPs. Ln^{3+} closer to the acceptors will exhibit higher FRET efficiencies. These results suggest that higher energy transfer from the UCNPs to the $CsPbBr_3$ QDs may be achieved for smaller donor sizes.

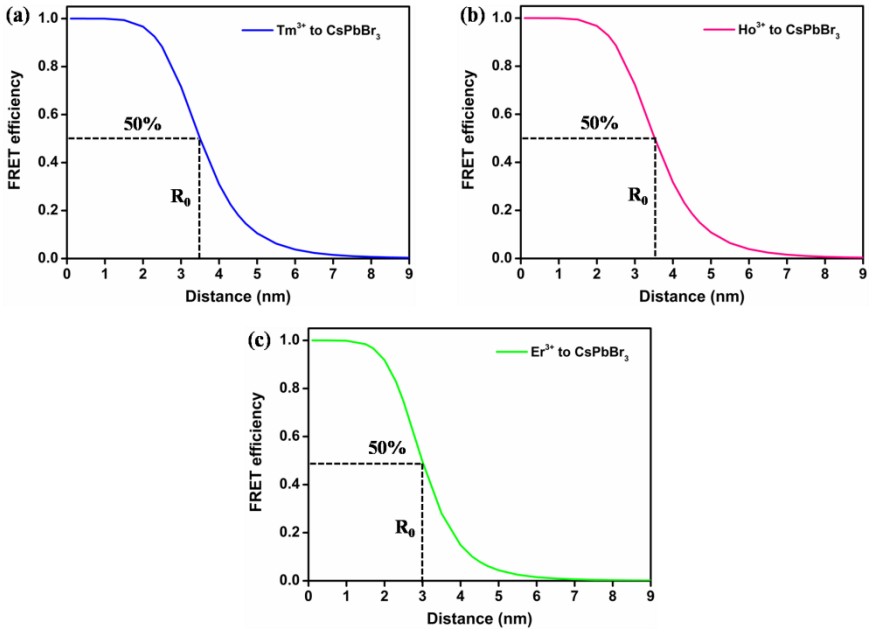

Fig. S8 FRET efficiency as a function of separation distance between the donor/acceptor pair: (a) Tm^{3+} to $CsPbBr_3$ QDs, (b) Ho^{3+} to $CsPbBr_3$ QDs and (c) Er^{3+} to $CsPbBr_3$ QDs.

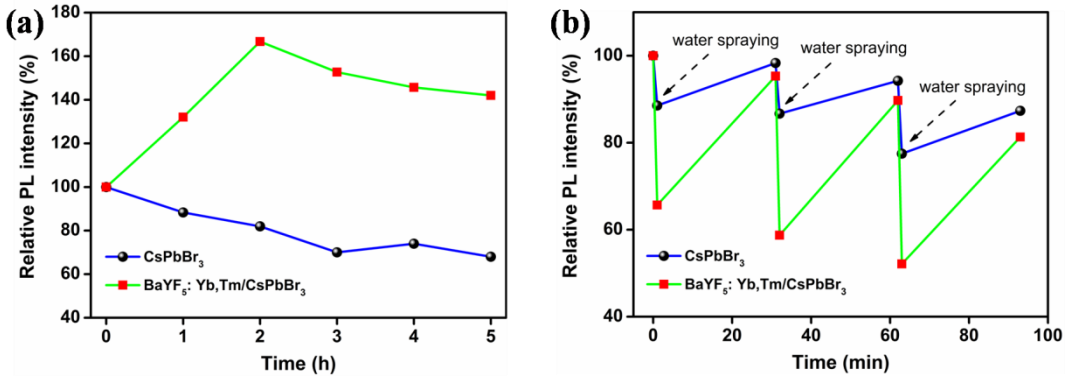

Fig. S9 (a) Thermal stability tests of the $CsPbBr_3$ QDs and $BaYF_5$: Yb, Tm/$CsPbBr_3$ composite films versus thermal treatment time at 80 °C under ambient pressure, (b) humidity stability tests. Exposure to moisture was realized by spraying deionized water onto the sample' surface.

Interestingly, the $BaYF_5$: Yb, Tm/$CsPbBr_3$ composite sample exhibited a sharp increase in PL intensity in the first two hours upon thermal annealing at 80 °C followed by a decrease, while the PL intensity was still enhanced by 42% after 5 h thermal treatment. On the contrary, an obvious thermal quenching of PL intensity was observed in the pristine $CsPbBr_3$ QDs sample and only 68% of the initial signal was left. It was also found that both the pristine $CsPbBr_3$ QDs and the $BaYF_5$: Yb, Tm/$CsPbBr_3$ composite displayed a slight red shift (1-2 nm) of emission, suggesting that the $CsPbBr_3$ QDs were growing during the thermal annealing process. Similar PL phenomena were also observed in the bare $CsPbBr_3$ QDs by Yuan *et al.*[13]

The PL changes observed in the $BaYF_5$: Yb, Tm/$CsPbBr_3$ composite are probably a result of the two competing processes: the increase of nonradiative recombination centers and the shortening of the distance between the energy donors and acceptors, which will lead to PL quenching and enhancement, respectively. Only the first process occurred in the pristine $CsPbBr_3$ QDs. The increase of the nonradiative recombination centers is likely arising from the partial loss of surface bonding ligands during the thermal treatment, followed by the formation of surface energy states and subsequent PLquenching.[13] On the other hand, the evaporation of cyclohexane is likely to favor a shorter distance between the energy donors and acceptors which will improve the FRET efficiency. Therefore, the PL intensity of the $BaYF_5$: Yb, Tm/$CsPbBr_3$ composite was enhanced due to the increased energy transfer efficiency from the energy donors to the acceptors. In the $BaYF_5$: Yb, Tm/$CsPbBr_3$ composite, the latter process dominated in the first two hours and then became weaker, accompanied with the PL enhancement and subsequent quenching.

The pristine $CsPbBr_3$ QDs and $BaYF_5$: Yb, Tm/$CsPbBr_3$ composite films were subjected to cycles of water spraying followed by natural drying (30 minutes in air) to investigate the stability to humidity of the materials and their PL performances. As shown in Fig. S8, the $BaYF_5$: Yb, Tm/$CsPbBr_3$ composite showed a serious PL intensity drop compared with the pristine $CsPbBr_3$ QDs upon water exposure. However, after 30 minutes drying, 87% and 81% of the original intensities were recovered after three cycles for the pristine $CsPbBr_3$ QDs and the $BaYF_5$: Yb, Tm/$CsPbBr_3$ composite, respectively. Further, the exciton peak positions of the two samples stayed the same. The PL quenching is probably associated with the desorption of the capping ligands on the surface of the nanoparticles or surface decomposition, followed by the occurrence of new surface trap states.[14] The $BaYF_5$: Yb, Tm/$CsPbBr_3$ composite is more sensitive to moisture compared with the pristine $CsPbBr_3$ QDs. In the $BaYF_5$: Yb, Tm/$CsPbBr_3$ composite, partial UCNPs detachment from the surface of the $CsPbBr_3$ QDs, owing to the desorption of the surface bonding ligands, or enhanced lanthanide vibrational quenching, could related to the reduced FRET efficiency and PL intensity in the presence of water.

References

1 X. Zhai, S. Liu, X. Liu, F. Wang, D. Zhang, G. Qin and W. Qin, *J. Mater. Chem. C*, 2013, **1**, 1525-1530.

2 I. O. P. D. Berti, M. V. Cagnoli, G. Pecchi, J. L. Alessandrini, S. J. Stewart, J. F. Bengoa and S. G. Marchetti, *Nanotechnology*, 2013, **24**, 175601.

3 Y. Lin, J. Jin and M. Song, *J. Mater. Chem. C*, 2011, **21**, 3455-3461.

4 M. Liu, L. Zhang, K. Wang and Z. Zheng, *CrystEngComm*, 2011, **13**, 5460-5466.

5 M. Zhang, H. Li, Q. Jing, Z. Lu and P. Wang, *Crystals*, 2017, **8**, 2.

6 B. Prevo and E. J. G. Peterman, *Chem. Soc. Rev.*, 2014, **43**, 1144-1155.

7 N. Hildebrandt, C. M. Spillmann, W. R. Algar, T. Pons, M. H. Stewart, E. Oh, K. Susumu, S. A. Díaz, J. B. Delehanty and I. L. Medintz, *Chem. Rev.*, 2016, **117**, 536-711.

8 W. R. Algar, D. Wegner, A. L. Huston, J. B. B. Canosa, M. H. Stewart, A. Armstrong, P. E. Dawson, N. Hildebrandt and I. L. Medintz, *J. Am. Chem. Soc.*, 2012, **134**, 1876-1891.

9 J.-C. Boyer and F. C. Van Veggel, *Nanoscale*, 2010, **2**, 1417-1419.

10 A. Bednarkiewicz, M. Nyk, M. Samoc and W. Strk, *J. Phys. Chem. C*, 2010, **114**, 17535-17541.

11 R. Marin, L. L. Paéz, A. Skripka, P. H. González, A. Benayas, P. Canton, D. Jaque and F. Vetrone, *ACS Photonics*, 2018, **5**, 2261-2270.

12 F. Artizzu, A. Serpe, L. Marchiò, M. Saba, A. Mura, M. L. Mercuri, G. Bongiovanni, P. Deplane and F. Quochi, *J. Mater. Chem. C*, 2015, **3**, 11524-11530.

13 X. Yuan, X. Hou, J. Li, C. Qu, W. Zhang, J. Zhao and H. Li, *Phys. Chem. Chem. Phys.*, 2017, **19**, 8934-8940.

14 S. Huang, Z. Li, B. Wang, N. Zhu, C. Zhang, L. Kong, Q. Zhang, A. Shan and L. Li, *ACS Appl. Mater. Interfaces*, 2017, **9**, 7249-7258.